THE ASTROPHYSICAL JOURNAL, 364:647–656, 1990 December 1

ON THE INTERPRETATION OF THE *EXOSAT* PHOTOMETRY OF TWO HOT DA WHITE DWARFS

STÉPHANE VENNES AND HARRY L. SHIPMAN
Department of Physics and Astronomy, University of Delaware
AND
ROBERT PETRE
Laboratory for High Energy Astrophysics, NASA/Goddard Space Flight Center
Received 1990 March 19; accepted 1990 June 1

ABSTRACT

The photometric observations by the *European X-Ray Observatory Satellite* (*EXOSAT*) using the Low Energy Detector of the hot DA white dwarfs GD 2 (WD 0004+330) and EG 70 (WD 1031−114) are analyzed assuming a number of hypotheses for the atmospheric structure and composition. The emission, photospheric in origin, is first interpreted using the simplest model in which the chemical composition is a homogeneous mixture of hydrogen and helium with various number ratios. For that purpose a new grid of model atmospheres is computed using as free parameters the effective temperature, the gravity, and the number ratio $N(\mathrm{He})/N(\mathrm{H})$. If the uncertainty on the effective temperature is large, then the atmospheres of EG 70 and GD 2 may be approximated by pure hydrogen compositions with an upper limit on the abundance of helium near 10^{-5} and 10^{-4}, respectively. Synthetic spectra with a representative sample of trace elements (C, N, Si) are calculated to constrain further the total amount of trace elements. Using both *EXOSAT* and *IUE* observations, we attempt to estimate simultaneously the effective temperature and the surface gravity of these stars. Assuming that the atmosphere is made of pure hydrogen and that a systematic +5% error affecting the *IUE* absolute flux is allowable, the atmospheric parameters of GD 2 are $T_{\mathrm{eff}} = 42{,}700$ K, $\log(g) = 8.0$. However, its high interstellar hydrogen column density ($N_{\mathrm{H}} > 5 \times 10^{19}$ cm^{-2}) may suggest the presence of a substantial reddening effect in the ultraviolet spectrum. In that case, the effective temperature is higher (near 50,000 K) than first estimated, and consequently some trace absorbers are needed to explain the EUV/soft X-ray measurement. It is known that helium diffuses on a very short time scale, leading to the formation of a chemical stratification configuration with the hydrogen layer floating on top of an helium envelope. Such stratified model atmospheres, described by the total mass of hydrogen along with the gravity and effective temperature, are used to inquire about the presence of a helium diffusive tail in the X-ray photosphere. We find that a high effective temperature of GD 2 must be accommodated with the *EXOSAT* data either with a thin hydrogen layer, or by an undetermined complex of metal opacities. The case for EG 70 leads to a much simpler picture with all observations accounted for by the atmospheric parameters $T_{\mathrm{eff}} = 25{,}800$ K, $\log g = 8.05$, and a pure hydrogen atmosphere. We examine the consequence of these conjectures on the spectral evolution theory of the white dwarf stars. Furthermore, we consider the accuracy of the model atmosphere calculations to assess the reliability of the conclusions.

Subject headings: stars: atmospheres — stars: white dwarfs — stars: X-rays — ultraviolet: general

I. INTRODUCTION

In an *EXOSAT* Guest Investigator program, we obtained soft X-ray photometric data on a number of hot DA white dwarfs in order to investigate further the chemical composition and atmospheric stratification of these objects. Since the first detection of thermal X-ray emission from the hot white dwarf Sirius B (see Shipman 1976), a picture has emerged in which some hot white dwarfs have pure hydrogen atmospheres and are strong X-ray emitters, and others emit far fewer X-rays than would be expected if they are pure hydrogen (Kahn *et al.* 1984; Petre, Shipman, and Canizares 1986; Jordan *et al.* 1987; Vennes *et al.* 1988; Paerels and Heise 1989; Koester 1989). In addition to providing a theoretical interpretation of the X-ray data, many of these papers make attempts to divine a pattern in the data and provide an explanation for these trends.

These studies basically show a trend for an increasing abundance of impurities (assumed to be helium) in the atmosphere with an increasing effective temperature of the hydrogen-rich DA white dwarf. Although there is a considerable debate on the reality of that correlation, there is at least two groups of DA white dwarfs discernible: a *cold* group ranging from 25,000 to 40,0000 K with a low or zero level of trace elements, and a *hot* group ranging from 45,000 to 65,000 K with an inferred mean He abundance of 10^{-3} relative to hydrogen by number.

A detailed study of the processes which can be responsible for that recognized fact was presented by Vennes *et al.* (1988). Two avenues retained the attention of these authors. First a new hypothesis requiring helium to be the complementary source of opacity to the hydrogen bound-free and electron scattering was proposed. After showing that the weak radiative support of helium does not account for the observations, they concluded that there is complete chemical separation of the hydrogen and helium layers. In that case, the helium will pollute the EUV/soft X-ray photosphere via ordinary diffusion only if the total mass of the overlying hydrogen layer is less than the mass of the photospheric layers of the DA white dwarf. That total mass of the hydrogen layer was found to

range roughly from $10^{-13}M_*$ at 25,000 K to $10^{-15}M_*$ at 65,000 K.

Discussing in a broader context the possible existence of a *thin layer* of hydrogen on the DA white dwarfs, Fontaine and Wesemael (1987) proposed a spectral evolution theory in which the statistics of the white dwarf classification and population is centered on the hypothesis that the total mass of hydrogen in *all* white dwarfs is linked to the hydrogen layer mass present in the DA white dwarfs. Some more arguments can also be found in Liebert, Fontaine, and Wesemael (1987). Apart from this, Vennes *et al.* (1988) recognized, as many authors have pointed out, that the additional opacity source may not be helium at all. This idea found support in the case of the DA Feige 24 (Vennes *et al.* 1989). In that case, the unique EUV spectrophotometric measurement by *EXOSAT* has been explained by the presence of a host of trace absorbers (10 elements from He to Ca), all present in the photosphere through the action of radiative forces.

The three pictures, a homogeneous distribution of hydrogen and helium in the photosphere, a stratified distribution of H and He and a homogeneous distribution of metals, are considered for the study of GD 2 and EG 70. The estimated temperature from Finley, Basri, and Bowyer (1990, hereafter FBB) places GD 2 (45,890 K) at the intersection of the cold group and the hot group, while EG 70 is in the cold group at 26,010 K, making it one of the coolest DA stars detected by *EXOSAT*. The EUV/soft X-ray data are compared extensively with the *IUE* data retrieved from the archives at NASA/GSFC. The magnitudes and colors are taken from McCook and Sion (1987). In the next section, we present the observations covering the entire spectral range for the hot DA white dwarfs. In § III, we detail the model atmosphere and synthetic spectrum calculations and we discuss the numerical accuracy of such calculations and the impact on the reliability of our results. Following this, in § IV, we derive the optimum atmospheric parameters that explain the complete spectral coverage. We finally review the current knowledge of the physics of the atmospheres of the hot DA white dwarfs (§ V).

II. OBSERVATIONS

Initially we planned to observe five hot DA white dwarf stars with *EXOSAT*. Restrictions on the mission lifetime limited us to four targets. One of our targets (WD 1615−154) was located very close to Sco X-1, and high background count rates caused the observation to be terminated with no useful data. Another target, WD 0109−264, has been reclassified as a subdwarf (Heber *et al.* 1984), and so it is not surprising that no X-rays were detected from it. This left us with two detections of GD 2 and EG 70. A very preliminary analysis of these detections was reported earlier by Petre and Shipman (1987).

The EUV/soft X-ray photometry of GD 2 and EG 70, reported by Petre and Shipman (1987), is coupled to the *IUE* ultraviolet spectrophotometry and to optical photometry. This allows us to construct a complete energy distribution for both DA stars covering all spectral regions of interest for these hot emitters. Table 1 summarizes the available observational material. The *EXOSAT* count rates were initially extracted using the automatic data analysis facility, but to reflect

TABLE 1

EXOSAT, *IUE*, AND OPTICAL OBSERVATIONS

A. *EXOSAT*

EG 70 (WD 1031−114)				GD 2 (WD 0004+330)			
Filter[a]	Date[b]	Exposure (s)	Rate (s^{-1})	Filter[a]	Date[b]	Exposure (s)	Rate (s^{-1})
3LX/LE1	85/348	3894	0.098 ± 0.006	3LX/LE1	85/353	1698	0.336 ± 0.018
AlP/LE1	85/348	5969	0.021 ± 0.002	AlP/LE1	85/353	8183	0.026 ± 0.002
...	...	...	...	B/LE1[c]	85/353	7259	0.016 ± 0.005

B. *IUE*

EG 70 (WD 1031−144)			GD 2 (WD 0004+330)		
Image	Date[b]	Exposure (s)	Image	Date[b]	Exposure (s)
SWP 30865S	87/120	1260	SWP 28884S	86/223	1200
SWP 30865L	87/120	1200	SWP 28884L	86/222	720
SWP 17014L	82/141	720	SWP 7456L	79/356	960
...	...	...	LWR 6460	79/356	1560

C. PHOTOMETRY

EG 70 (WD 1031−114)					GD 2 (WD 0004+330)		
Johnson			Strömgren		Johnson		
U	*B*	*V*	*u*	*y*	*U*	*B*	*V*
11.80	12.82	12.97	12.89	13.00	12.32	13.53	13.82

[a] On *EXOSAT* telescope Low Energy 1, 3LX: thin lexan; AlP: aluminium/parylene-N; B: boron.

[b] Epoch of observation given in year/day format as presented in *IUE* and *EXOSAT* observation logs.

[c] Boron count rate multiplied by a factor of 4.

improvement in the knowledge of the *EXOSAT* calibration we use the count rates currently available in the *EXOSAT* data base. The quoted errors are at the 1 σ level. The well-documented obscuration factor of the Low Energy Detector is absorbed in the effective area function. However, the boron count rate for GD 2 should be used cautiously. It has been discovered that unexpected scattering in the boron filter broadens the PSF (point-spread function) and leads to an underestimate of the count rate by a large factor. This effect has not been taken into account during the acquisition of the data, and we chose to arbitrarily multiply the boron count rate by a factor of 4 in the subsequent analysis. The count rates for the Lexan 3000 and Al/P filters have been checked for ultraviolet contamination. Paerels and Heise (1989) have determined, in a EUV/soft X-ray survey of 21 hot DA white dwarfs, that ultraviolet contamination does not critically affect the determination of the atmospheric parameters of those stars. Our own estimate of the *UV* contamination in the case of GD 2 and EG 70 using the simple recipe given in the *EXOSAT Observers Guide Part I/II* (revision 2) confirmed that the ultraviolet contribution to the count rates is much smaller than the 1 σ errors.

We acquired the *IUE* short wavelength (SWP), both small (S) and large aperture (L), and long wavelength (LWR) images using the Data Analysis Facility at NASA/Goddard Space Flight Center. The small aperture version of the SWP image is intended for use in the analysis of the Lyα line profile because it suppresses the Lyα geocoronal emission. The images have been subsequently corrected for wavelength shift (Thompson 1988) and for time degradation using the prescription of Bohlin and Grillmair (1988) for the entire spectral range (1150–3200 Å). However, because their tables do not extend to the exposure date of the small and large aperture images of EG 70 (SWP 30865, year = 1987.329) we simply used the corrections for the more recent epoch (S: 1987.11, L: 1986.89). An inspection of the tables reveals that, for most of the wavelength bins, the resultant flux is not affected by more than a few percent. Finley, Basri, and Bowyer (1990), in conducting an ultraviolet continuum flux survey of the hot DA stars, found that a systematic flux distortion in the range 1320–3200 Å relative to theoretical spectra is still present, even after applying all known corrections. Holberg, Wesemael, and Basile (1986, hereafter HWB) found a similar result for the Lyα region, but unfortunately prior to the development of the correct algorithm to account for the time degradation. However, it is interesting to note that the Lyα blue wing, which is depleted in uncorrected spectra relative to theoretical line profiles, behaves correctly after applying time degradation corrections. We thus applied the FBB flux corrections to the relevant range (1320–3200 Å) and no further corrections to the Lyα range (1150–1320 Å).

We present in Figures 1 and 2 a composition of the *IUE* short-wavelength large- and small-aperture spectra of EG 70 and GD 2, respectively. The absolute flux scales of the small-aperture exposures were recovered by dividing the corrected large-aperture image by its corresponding corrected small-aperture image. It is found that, in the vicinity of the Lyα line, the true flux scale of the image SWP 28884S is obtained by using a factor of 3.23 while a factor of 3.40 is necessary for the image SWP 30865S. There is no significant wavelength dependance of these factors in a 100 Å range across Lyα. The flux distributions of EG 70 and GD 2 show a slight increase shortward of the 1320 Å cutoff of the FBB correction tables. This

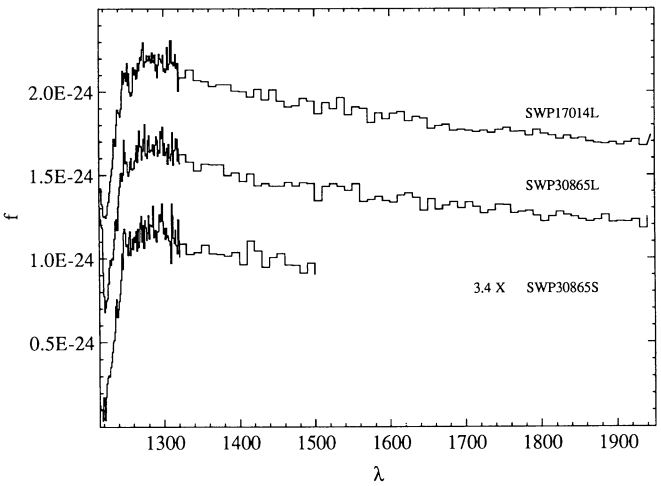

FIG. 1.—Far-ultraviolet energy distribution, f_ν (ergs cm^{-2} s^{-1} Hz^{-1}) vs. λ (Å), of the DA white dwarf EG 70. The *IUE* spectra SWP 17014L (shifted upward by 1 × 10^{-24}), SWP 30865L (shifted upward by 5 × 10^{-25}), and SWP 30865S are binned at 10 Å intervals for $\lambda > 1320$ Å and are presented at their original binning for $\lambda < 1320$ Å.

justifies, in the analyses of the Lyα profile of GD2, the addition of an ad hoc 0.91 lowering factor to the SWP 28884 small-aperture spectrum and a 0.94 lowering factor to the SWP 30865 small-aperture spectrum. The application of these factors should be considered as a preliminary attempt to extend the correction factors of FBB to the Lyα range. Finally, we complete the energy distribution by the use of wide-band magnitudes U, B, and V and Strömgren magnitudes listed in McCook and Sion (1987) which were converted to absolute flux using the relations developed by Heber *et al.* (1984). The magnitude $m_\lambda = 0.0$ is defined by $f_\lambda = 4.16 \times 10^{-9}$, 6.17×10^{-9}, and 3.58×10^{-9} ergs cm^{-2} s^{-1} Å^{-1} for the U, B, and V filters, respectively, and by $f_\lambda = 1.146 \times 10^{-8}$ and 3.6×10^{-9} ergs cm^{-2} s^{-1} Å^{-1} for the Strömgren u and y filters, respectively. Magnitudes are useful in determining the value of R/D, where R is the radius of the white dwarf and D its distance; this parameter can relate the theoretical Eddington flux to the observed flux.

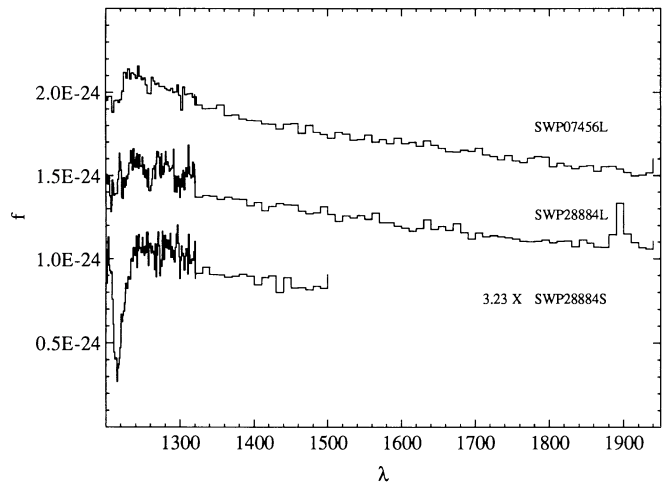

FIG. 2.—Same as Fig. 1 but for GD 2 and the *IUE* spectra SWP 7456L, SWP 28884L, and SWP 28884S shifted upward accordingly.

III. THE MODEL ATMOSPHERES AND SYNTHETIC SPECTRA

a) *The Model Atmosphere Calculations*

The model atmosphere calculations performed in this study make use of a program developed after the pioneering code of Auer and Mihalas (Mihalas, Heasley, and Auer 1975). The central characteristic of the solution procedure involves the complete linearization of the set of equations describing a stellar atmosphere, namely the equation of radiative transfer, the equations of hydrostatic, radiative, and statistical equilibrium, and two relations to ensure charge neutrality and the conservation of the total number of particles. The geometry of the atmospheric layers is plane parallel, and the statistical equilibrium of the constituents is obtained assuming local thermodynamic equilibrium (LTE). Although Koester and Herrero (1988) have shown that high-dispersion spectroscopy of the hydrogen Hα line of some hot DA stars reveals the onset of a non–LTE core, the use of the low-dispersion mode with *IUE* smooths out the sharp non–LTE core of Lyα so that the core affects only marginally the overall shape of the line.

The study of white dwarf atmospheres has also led to the exploration of a new possible compositional structure, replacing the standard homogeneous composition (Jordan and Koester 1986; Vennes *et al.* 1988; Vennes, Fontaine, and Wesemael 1989; Koester 1989). A nonuniform distribution of elements (H, He in the present case) may be determined self-consistently by solving the equilibrium diffusion equation along with the other atmospheric structural equations. Because the static diffusion equation depends only on the mean ionic charges at each depth (approximately constant through the transition zone) and on the independent Lagrangian variable m (the mass loading in g cm^{-2}), the convergence of the atmospheric structure is secured easily even in the presence of a strong compositional gradient at the interface of the H and He layers. The only other major modification to the Auer-Mihalas method involves a more intimate coupling between the transfer equation and the radiative equilibrium equation. This allows the convergence to reach a total flux constancy at each depth of better than 1 part in 10,000 using a small number of iterations (<10) and a reasonable number of depth points (<100). More details will be presented elsewhere (Vennes, Fontaine, and Wesemael 1990; but see also Vennes 1988).

In the present study, GD 2 and EG 70 are modeled with an extension of two hydrogen line–blanketed grids of model atmospheres computed for an analysis of the EUV/soft X-ray photometry from *EXOSAT* of 15 DA white dwarfs presented by Vennes, Fontaine, and Wesemael (1989). The two grids, one of homogeneously mixed hydrogen and helium and the other assuming a stratified H/He configuration, are now respectively extended to the range of parameters: log He/H $= -10, -6, -5, -4, -3, -2$; log $M_{\rm H} = -13.0, -13.5, -14.0, -14.5, -14.75, -15.0, -15.25, -15.5$. The effective temperature now covers $T_{\rm eff} = 25$, 30, 35, 40, 45, 50, 55, 60, and 65×10^3 K. A surface gravity $g = 10^8$ cm s^{-2} is assumed. A third grid of models is specifically calculated for the study of the Lyα line profile in both GD 2 and EG 70. This grid of pure hydrogen models covers the range of temperature from 22,000 to 50,000 K at each of five surface gravity values, log $g = 7.0$, 7.5, 8.0, 8.5, and 9.0.

b) *Accuracy of the Models*

The numerical accuracy of model atmosphere calculations has been questioned in studies involving precise spectrophotometric measurements of the EUV/soft X-ray spectra of the hot DA stars Sirius B and HZ 43 by *EXOSAT* (Paerels *et al.* 1988; Heise *et al.* 1988). The reason is that a comparison of their theoretical EUV/soft X-ray fluxes with those provided in earlier investigations (Wesemael *et al.* 1980; Petre, Shipman, and Canizares 1986) reveals discordance at a 10% level at 50,000 K and even much higher at 30,000 K ($>50\%$). Heise *et al.* (1988) were specifically concerned with the difficulty in obtaining a formal fit to the *EXOSAT* spectrum of HZ 43 which is consistent with the atmospheric parameters derived from *UV* spectral range (Holberg, Wesemael, and Basile 1986) and with the low interstellar hydrogen column density measured from EUV *Voyager* observations (Holberg *et al.* 1980).

The numerical treatment as well as approximations to the basic physics can influence the final output of a model atmosphere calculation, the synthetic spectrum. Because the atomic physics of the dominant constituent of our models, the hydrogen atom, is known with great accuracy, we focus on the numerical aspects of the problem. But it should be mentioned that the hydrogen ionization balance at depth is likely to be affected by the lowering of the ionization potential. Using a Debye-Hückel perturbation model, Heise *et al.* (1988) found a significant effect on the soft X-ray emission of a model suitable for the DA star HZ 43.

Variations of the trace element abundances modify the temperature structure of the atmosphere. The hydrogen line profiles, which are formed in a broad range of depths, have a dependence on trace element abundances through this temperature effect. We test the effect of the helium diffusive tail in the H/He stratified models on the hydrogen Lyα line profile. At two selected wavelengths, 1215 and 1235 Å, for the sequence of stratified models at $T_{\rm eff} = 50{,}000$ K and log $g = 8$, the flux normalized at the V magnitude is increased by 2.6% (1215 Å) and 1.2% (1235 Å) if the hydrogen layer mass is decreased from $10^{-13.5}$ to $10^{-14} M_*$. The variation between 10^{-13} and $10^{-13.5} M_*$ is negligible. This effect corresponds to a temperature increase of 800 K for a sequence of pure hydrogen models near 50,000 K. It indicates also that any analysis of the Lyα profile of hot DA white dwarfs with a hydrogen layer mass inferred from EUV/soft X-ray data less than $10^{-14} M_*$, should be conducted self-consistently instead of using a grid of pure hydrogen models. For models with a hydrogen layer mass greater than $10^{-14} M_*$, the departure from a pure hydrogen model decreases rapidly, and consequently this assumption can be made.

The numerical treatment itself dominates the accuracy of the EUV/soft X-ray synthetic spectra calculation through the effect on the temperature structure of the model. Both the frequency grid, used to define the total flux at each depth of the model atmosphere, and the depth grid itself need to be carefully constructed to avoid any flux errors greater than 1%. We conducted a few tests at $T_{\rm eff} = 30{,}000$ and 50,000 K that reveal that at least 70 depth points need to be defined between log $\tau_R = -7$ and log $\tau_R = 2$ and that the error on the flux is less than 1% using 100 depth points. The high-energy spectrum needs to be mapped densely down to 50 Å to integrate correctly the total flux. We can generally state that for wavelengths longer than 80 Å our synthetic spectra are precise at a 1% level, as secured by a comparison with the fluxes of the 50,000 K model from Heise *et al.* (1988), and that the error introduced by the model atmosphere calculation in the subsequent analysis is negligible.

c) The Synthetic Spectra

The model atmosphere temperature and density structures are used to calculate synthetic spectra with detailed and specific frequency grids. A first grid covers the EUV/soft X-ray spectral range between 20 and 500 Å. A second grid is specifically applied to the hydrogen Lyα line between 1100 and 1400 Å. The last grid covers sparsely the ultraviolet/optical region between 1100 and 6000 Å. In the EUV/soft X-ray spectral range, the He II Lyman lines are particularly important in the calculation of the predicted *EXOSAT* count rates. We use a version of the Auer and Mihalas (1972) hydrogenic line broadening recipe corrected for some misprint errors. The Lyα line profile is calculated using a procedure provided by Deane Peterson (private communication) that makes use of appropriate interpolation functions in the tables of Vidal, Cooper, and Smith (1973). The carbon, nitrogen and silicon bound-free opacities for the ions C III, C IV, N III, N IV, N V, and Si IV are also included for the calculation of the synthetic spectra.

IV. ANALYSIS AND RESULTS

The analysis consists of an extensive modeling of the available observational data for the hot DA white dwarfs GD 2 and EG 70. The EUV/soft X-ray spectral range is analyzed using different hypotheses for the chemical structure of the DA atmosphere: homogeneous and stratified H/He composition, and homogeneous CNSi/H composition. To analyze the UV continuum and the Lyα profile we take advantage of the upper limits on trace elements obtained in the analysis of the *EXOSAT* data (see next section). The inferred upper limits on the abundance of trace elements affect only slightly (<2%) the emergent optical-*UV* flux. For the analysis of the Lyα profile and continuum flux, we consider only a grid of pure hydrogen models defined in the $T_{\rm eff}$–log g space of parameters. In the following, all theoretical spectra are normalized to the observed optical flux characterized by the V magnitudes m_V = 13.0 and 13.82 for EG 70 and GD 2, respectively.

a) Constraints Derived from the EXOSAT Data

The high-energy spectrum of a hot DA star observed at Earth is dependent on the actual stellar atmospheric chemical structure, gravity, and effective temperature. The effect of the interstellar medium through bound-free absorption by neutral hydrogen and helium is quantified by the neutral hydrogen column density ($N_{\rm H}$ cm^{-2}) in the line of sight with the other elements scaled to the cosmic abundance ratios. We use the interstellar absorption cross section ($\sigma_\nu^{\rm ism}$) of Morrisson and McCammon (1983). The theoretical spectra are scaled to the absolute flux observed at Earth by means of the V magnitude. The predicted count rate is defined by the relation

$$c(\mathrm{s}^{-1}) = 4\pi \frac{R^2}{D^2} \int \frac{H_\nu}{h\nu} A_\nu e^{-\tau_\nu^{\rm ism}} d\nu \,, \qquad (1)$$

where R and D are the radius and distance of the star, H_ν is the Eddington flux, and $\tau_\nu^{\rm ism}$ is the interstellar optical depth given by $N_{\rm H}\sigma_\nu^{\rm ism}$. A_ν is the filter effective area function. The solid angle is defined by the magnitude V

$$4\pi \frac{R^2}{D^2} = \frac{f_V}{H_V} \,, \qquad (2)$$

where H_V is the model Eddington flux at 5500 Å and f_V is the observed absolute flux given by the magnitude V:

$$\log_{10} f_V = -0.4 m_V - 19.443 \,. \qquad (3)$$

The count rates for each filter are calculated in a two-dimensional grid with $N_{\rm H}$ as a function of a given parameter, $T_{\rm eff}$, log He/H, log CNSi/H or log $M_{\rm H}$. The surface gravity and the complementary parameter are held fixed during that procedure. Contours of equivalent likelihood are interpolated and graphically displayed allowing a visual inspection for the determination of the optimal parameters.

The results of this analysis, using representative parameters, are presented in Figures 3 and 4 for EG 70 and GD 2, respec-

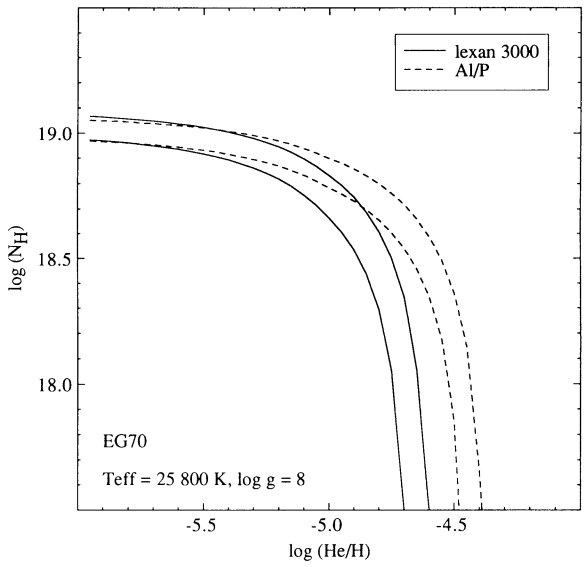

FIG. 3*a*

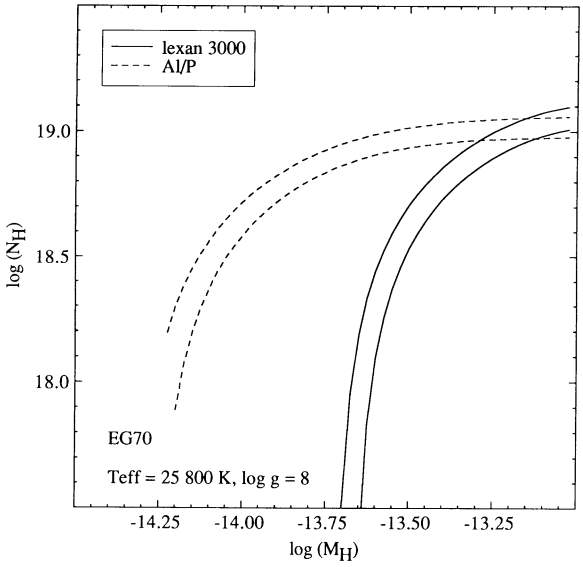

FIG. 3*b*

FIG. 3.—(*a*) Equal likelihood contour curves (1 σ) for the *EXOSAT* count rates (lexan 3000 and Al/P) of EG 70 in the log (He/H)–log ($N_{\rm H}$) plane. The independent atmospheric parameters are $T_{\rm eff}$ = 25,800 K and log g = 8. (*b*) Same as (*a*) but in the plane log ($M_{\rm H}$)–log ($N_{\rm H}$).

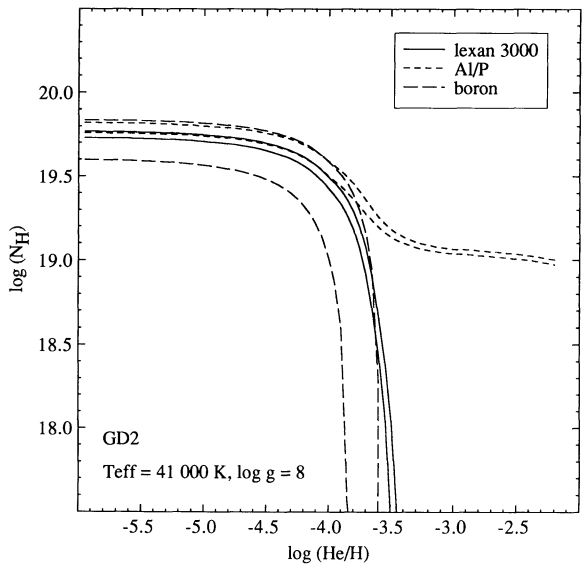

FIG. 4a

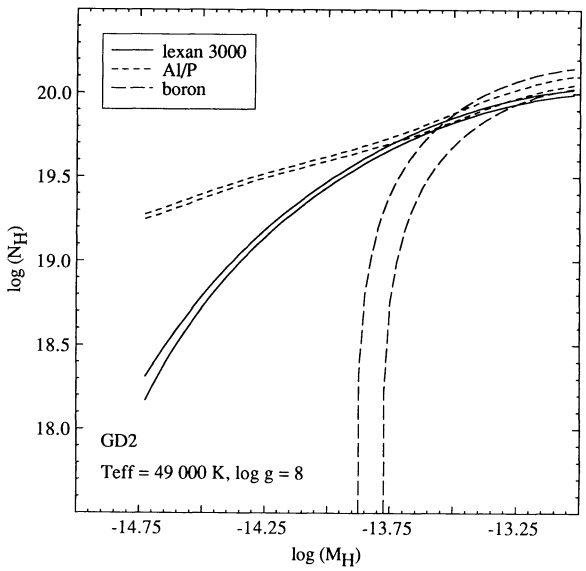

FIG. 4b

FIG. 4.—(*a*) Equal likelihood contour curves (1.5 σ, 1 σ for boron) for the *EXOSAT* count rates (lexan 3000, Al/P, and boron) of GD 2 in the log (He/H)–log(N_H) plane. The independent atmospheric parameters are T_{eff} = 41,000 K and log g = 8. (*b*) Same as (*a*) but in the plane log (M_H)–log (N_H) and using the atmospheric parameter T_{eff} = 49,000 K.

tively, the overlapping between all filter contour curves determines the region of equally acceptable solutions. Contour curves are defined by 1.5 σ error for GD 2 and 1 σ error for EG 70. Table 2 summarizes the best solutions obtained for a wide range of possible effective temperatures. The symbols M_H, He/H, and CNSi/H represent the mass of the superficial hydrogen layer, the homogeneous helium abundance relative to hydrogen by number, and the metal (C, N, and Si) abundances, respectively. On the right of each of the columns labeled by log M_H, log He/H, or log CNSi/H, are the associated values of log N_H. It appears that in allowing a large uncertainty on the atmospheric parameter T_{eff}, the issue of the determination of the chemical composition is quite inconclusive. At the upper range of temperature, we may report the detection of the diffusive tail of helium in the EUV/soft X-ray photosphere. In the context of the homogeneous models, an equivalent conclusion is reached with the nonzero helium abundance inferred from the hottest model for EG 70. But in that context GD 2 is only consistent with pure hydrogen models provided the effective temperature is lower than 43,000 K at log g = 8. We need to constrain further the atmospheric parameters, T_{eff} and g, to determine uniquely the abundance pattern. Fortunately, the maximum departure from a pure hydrogen atmosphere is mild enough, as witnessed by Table 2, that we may use the grid of pure H models to interpret the *IUE* data.

b) Method of Analysis of the Continuum Flux and Lyα *Profile*

In this analysis we follow a similar approach to that of Holberg, Wesemael, and Basile (1986) for both the Lyα line profile and the UV continuum. Despite the fact that the

TABLE 2

RESULTS OF THE EUV/SOFT X-RAY ANALYSIS

A. GD 2 (WD 0004+330)

T_{eff} (K)	log g	log M_H[a]	log N_H[b]	log He/H	log N_H	log CNSi/H	log N_H
40,000.....	8	> −13.30	19.7	< −4.3	19.7	< −6	19.7
43,000.....	8	> −13.50	19.8	< −4.0	19.8	< −6	19.8
46,000.....	8	−13.40	19.9	...	...	...	...
49,000.....	8	−13.50	20.0	...	...	...	...

B. EG 70 (WD 1031−114)

T_{eff} (K)	log g	log M_H	log N_H	log He/H	log N_H
24,500.....	8	...	...	...	...
25,000.....	8	> −13.15	18.8	< −5.7	18.8
25,500.....	8	> −13.25	19.0	< −5.0	19.0
26,000.....	8	> −13.35	19.1	< −4.8	19.1
26,500.....	8	−13.25	19.1	< −4.7	19.2
27,000.....	8	−13.35	19.2	−4.7	19.2

[a] M_H in stellar mass unit M_*.

[b] log N_H (N_H in cm^{-2}) is given at the largest value over the range of acceptable solutions.

analysis of the Lyα line is not totally independent of the continuum flux analysis, we proceed to it separately. The synthetic spectra of the Lyα lines are submitted to a χ^2 test to evaluate the likelihood of each element in the ($T_{\rm eff}$, g) grid of models. The contour curves of equal χ^2 are interpolated in that grid. A difficult aspect of this analysis is to deal correctly with the intrinsic statisical fluctuation of the spectrum. Because there is no *a priori* knowledge of the noise present at each bin of a given image, the statistical weight of each bin is evaluated with the standard deviation of the spectrum relative to an arbitrary function. Ultimately the best comparison function should be the optimal solution itself. However, for the Lyα lines we follow a simple approach by estimating the standard deviation relative to a linear least-squares fit of the continuum flux on each side of the line. The standard deviation at intermediate bins is evaluated by interpolating between the two delimiting values. In the case of the continuum flux analysis, the standard deviation is evaluated the same way in a series of consecutive bins of 40 Å width. We define the 1 σ contour of equal χ^2 by

$$\chi^2_\nu(1\ \sigma) = \chi^2_\nu(\min) + \frac{1}{\nu} \tag{4}$$

$$\nu = \frac{W(\text{Å})}{\Delta(\text{Å})} - 3\ , \tag{5}$$

where χ^2_ν is the reduced χ^2 and ν is the number of free parameters in a bidimensional analysis. W(Å) is the width of the spectral range considered for the χ^2 and Δ(Å) is the resolution of the spectrum ($\Delta_{1/e}$ = 7.0 Å, FWHM = $\Delta_{1/2}$ = 5.75 Å). The ranges chosen for the analysis of the Lyα line are 1170–1275 Å and 1150–1310 Å for GD 2 and EG 70, respectively. The relative weight of the line and the continuum is then approximately equal in both analyses. The wavelength range for the analysis of the UV continuum flux alone is 1320–1950 Å and can be extended to 1320–3100 Å for GD 2. When applied to the Lyα profile of two previously studied cases, the DA stars GD 153 and CD −38°10980 (HWB), this method provides consistent results. The set of parameters ($T_{\rm eff}$, log g) obtained using a digitized version of Figures 4*a* and 4*b* of HWB, with the same normalization procedure, is for GD 153 (42,500 ± 2000, 8.1 ± 0.5). This result is not significantly different from HWB (42,375 ± 1480, 8.23 ± 0.3). Our broader range of acceptable solutions follows our method for estimating the noise, which gives higher estimates than HWB. Our solution for CD −38°10980 (24,800 ± 200, 8.1 ± 0.2) is also consistent with HWB (24,500 ± 140, 8.08 ± 0.15).

The solid angle sustained by the star is determined using two complementary approaches. A first method, which is model-independent, normalizes the theoretical flux to an arbitrary bin of the observed spectral region itself. This withdraws all *absolute* photometric information from the subsequent analysis and only *relative* photometric information remains, i.e., the shape of the spectrophotometric measurement. A strong dependence on the model effective temperature and on the absolute photometric measurements is introduced in the solid angle determination by applying the normalization to another spectral region significantly independent of the spectral region under scrutiny. The V magnitude, using relations (2) and (3), provides such an independent pivot. The first method, applied to the Lyα lines, generates *all* acceptable solutions in the ($T_{\rm eff}$, g) space of parameters, independently of other spectral regions, and depicts the strong correlation between $T_{\rm eff}$ and g. A normalization to the V magnitude introduces a strong dependence on the effective temperature and no further dependence on the surface gravity. This last method simply brings to the determination of the stellar parameters the information already contained in the continuum flux analysis. This is what is behind the excellent correspondence reached by two complementary studies, one on the continuum flux alone (FBB) and one on the Lyα range (HWB). In the next section we merge the results of the Lyα/continuum analysis with the constraints derived from the *EXOSAT* data.

c) *Optimal Solution to the EXOSAT and IUE Data*

There are now two plausible schemes that explain the complete spectrum of both GD 2 and EG 70. A first one, requiring that these two DA stars lie in the lower part of the temperature range defined in Table 2, implies that the chemical composition of their atmospheres is pure hydrogen. If the temperature is found to be higher, the presence of trace absorbers is required. This circumstantial behavior is simply explained by the necessity to suppress the excess of high-energy flux produced by higher temperature models relative to the *EXOSAT* observations.

We now follow two different approaches: we may maintain the chemical composition as a free parameter, or we may consider *a priori* that there are no trace elements. For that purpose, we need to reanalyze the *EXOSAT* data with the pure hydrogen grid of models in the space of parameters ($T_{\rm eff}$, g) instead of using the [$T_{\rm eff}$, ($M_{\rm H}$, He/H, or CNSi/H)] grids of models. This new analysis reveals an extremely useful circumstance: the behavior of the EUV/soft X-ray emission in the ($T_{\rm eff}$, g) space of parameters is orthogonal to the behavior of the Lyα line profile. On the other hand, if we maintain the chemical composition as a free parameter, the determination of the effective temperature relies only on the Lyα/continuum analysis. It is important to note that except for an exploratory 95% adjustment factor on the GD 2 *IUE* spectra we do not consider the overall calibration uncertainty of the *IUE* absolute flux scale. The 1 σ error contours defined in the previous section account only for the intrinsic statistical quality, the χ^2 test, of a given model compared to the data. The effect on the solution of a global 5% shift of the measurements is explored by applying a 0.95 reduction factor to the *IUE* ultraviolet flux of GD 2.

Figures 5 and 6 show the combination of the analyses of the *EXOSAT* and *IUE* data for EG 70 and GD 2 using the grid of pure hydrogen models and a certain subset of *IUE* images, as defined in the legends. The *EXOSAT* contour curves are defined by the quadratic sum of the errors for each of the filters (2.1 σ for GD 2 and 1.4 σ for EG 70), and the *IUE* contour curves are defined by a 1 σ error. We have adjusted the ad hoc correction factors such that the results of the *IUE* continuum analysis are always consistent with the *IUE* Lyα analysis but the continuum analysis provides a significantly narrower range of acceptable models. This follows simply from the fact that large-aperture images (used for the continuum) are of better quality than small-aperture images (used for Lyα) and that a larger number of independent data are used in the continuum flux analysis. We display only the results of the Lyα analysis, which provides a conservative estimate of the errors. As witnessed by Figure 5, the range of acceptable solutions with the *IUE* data alone is restrictive enough that we can accept the hypothesis that there are no trace elements in EG 70. We see that following this suggestion the *EXOSAT* data in the context

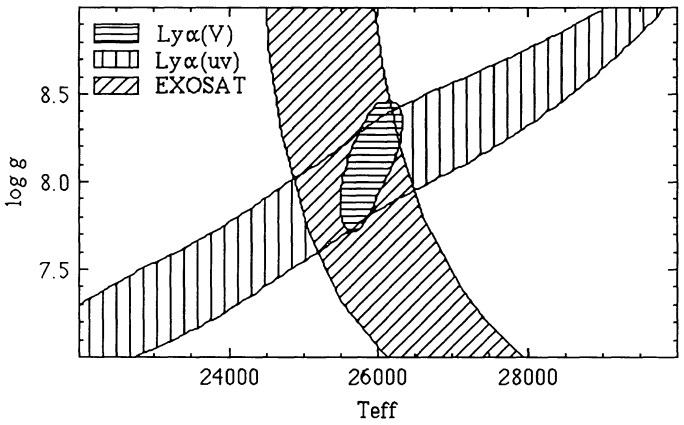

FIG. 5.—Equal likelihood contour curves for the EUV/soft X-ray count rates analysis (labeled *EXOSAT*), the Lyα line profile analysis normalized at 1300 Å (labeled uv), and the Lyα line profile analysis normalized to the magnitude *V* (labeled V) for the DA star EG 70 using pure hydrogen models in the plane $T_{\rm eff}$–log *g* and the *IUE* image SWP 30865S.

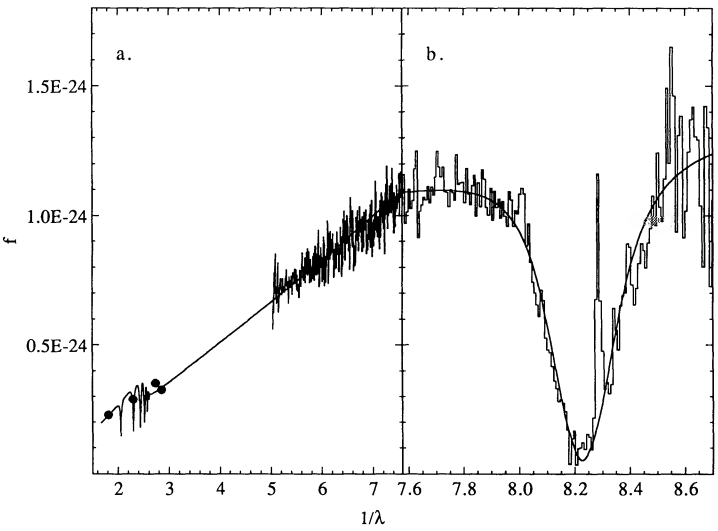

FIG. 7.—Complete ultraviolet/optical distribution (f_ν vs. λ^{-1} μm^{-1}) of the DA star EG 70 compared to a synthetic spectrum of a model atmosphere with the parameters $T_{\rm eff}$ = 25,800 K, log *g* = 8.05. Panel (*a*) contains the Johnson *U* and *B* magnitudes, the Strömgren *u* and *y* magnitudes, and the *IUE* image SWP 30865L. Panel (*b*), drawn with an expanded abscissa, contains the *IUE* image SWP 30865S (the flux scale is adjusted by a total factor of 0.94 × 3.4 = 3.196).

of pure hydrogen models are consistent, inside 1 σ error bars for all available data, with the solution ($T_{\rm eff}$, log *g*) = (25,800 ± 400, 8.05 ± 0.4). This solution is compared to the optical and ultraviolet data in Figure 7. In the same context, the solution for GD 2 is a small overlapping area ($T_{\rm eff}$, log *g*) = (40,500–44,000, 7.4–8.2) using a lowering factor of 0.91 for the Lyα range to correct for the discontinuity found at 1320 Å and an additional exploratory 0.95 factor for the entire *IUE* spectral range (Fig. 6). If we exclude the *EXOSAT* results for the pure hydrogen models from the ($T_{\rm eff}$, *g*) analysis and if we consider the lowering factor of 0.91 on Lyα alone, the solution is ($T_{\rm eff}$, log *g*) = (46,100 ± 2500, 8.2 ± 0.5), and in that case the best solution for the chemical composition is a stratified model at log $M_{\rm H}$ = −13.4 ± 0.1 or a model with an unidentified complex of metals. However, if we consider another subset of *IUE* images the solution for GD 2 can be appreciably modified. The continuum flux analysis of the images SWP 7456 and LWR 6460 provides a lower temperature, $T_{\rm eff}$ = 43,100 K (log *g* = 8), corresponding to a solution we already obtained by reducing the flux of the image SWP 28884 by 5%. A similar exercise for EG 70, using the image SWP 17014, provides a solution, $T_{\rm eff}$ = 25,500 K (log *g* = 8) consistent with our first estimate. This means that unless we consider the effect of a systematic 5% calibration excess of the *IUE* flux on a particular image, the hydrogen-rich atmosphere of GD 2 is likely to contain trace elements. An analysis of the *IUE* high-resolution spectrum of GD 2 may well be an indicator of the presence of metals like C, N or Si in the photosphere of that star.

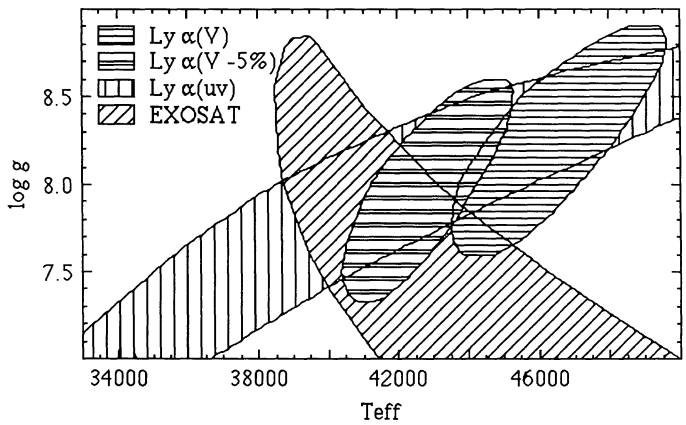

FIG. 6.—Same as Fig. 5 but for the DA star GD 2 using the *IUE* image SWP 28884S. The complementary label −5% refers to the exploratory reduction factor applied to the *IUE* images of GD 2.

The case for trace elements in GD 2 is even stronger if we take a look at the high interstellar hydrogen column density $N_{\rm H}$ inferred from all models in Table 2. $N_{\rm H}$ is often linked to another important parameter describing the interstellar medium, the extinction coefficient E_{B-V}, through a linear relationship $N_{\rm H} = 6 \times 10^{21} E_{B-V}$ mag^{-1} cm^{-2} (Spitzer 1978, pp. 3, 156). It appears that, in applying the Seaton (1979) extinction law to our synthetic spectra and a conservative value of the column density log $N_{\rm H}$ = 19.6 (E_{B-V} = 0.0065), the solution to the Lyα/continuum analysis of GD 2 is increased from $T_{\rm eff}$ = 46,100 to 49,200 K. Although the relationship between $N_{\rm H}$ and E_{B-V} shows a considerable scatter at this low value of the extinction coefficient, it is possible that any DA star lying near the Galactic plane like GD 2 (b = −27°) with a large interstellar hydrogen column density may be affected by a noticeable ultraviolet extinction. On the other hand, the effect of a large interstellar hydrogen column density on the core of the Lyα line is not clear, depending on the physical state prevailing in the interstellar medium. In Figure 8, we present the optical/ultraviolet synthetic spectrum at $T_{\rm eff}$ = 46,100 K and log *g* = 8.2 compared to the *IUE* data and optical magnitudes of GD 2.

To recapitulate the results of our analyses, we find that the DA white dwarf EG 70 is best modeled by a pure hydrogen model atmosphere at $T_{\rm eff}$ = 25,800 K and a surface gravity of 1.1 × 10^8 cgs. The DA white dwarf GD 2 is, assuming a reasonable uncertainty on the interstellar optical/*UV* extinction and on the *IUE* absolute flux calibration, lying between $T_{\rm eff}$ = 42,700 K (log *g* = 8.0, pure hydrogen, no extinction, −5%

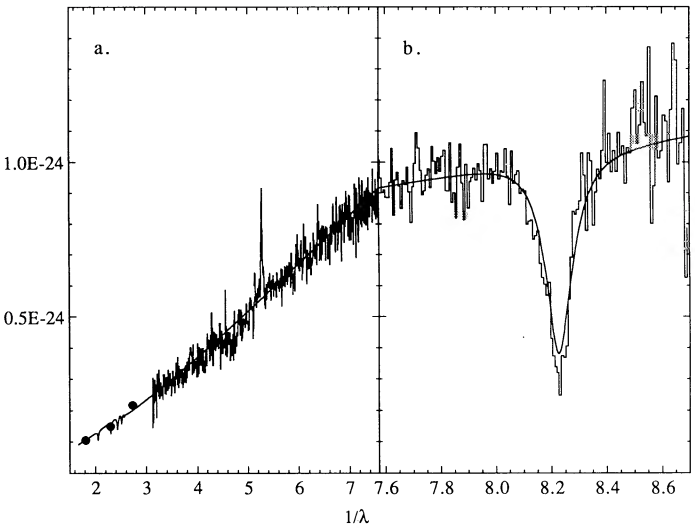

FIG. 8.—Same as Fig. 7 but for GD 2. The model atmosphere parameters are $T_{\rm eff}$ = 46,100 K and log g = 8.2. The *IUE* images depicted in panel (*a*) are LWR 6460 and SWP 28884L together with the Johnson *UBV* magnitudes, and the image in panel (*b*) is SWP 28884S (the flux scale is adjusted by a total factor of 0.908 × 3.23 = 2.935).

ultraviolet flux correction) and 49,200 K (log g = 8.5, stratified/metals atmosphere, E_{B-V} = 0.0065).

V. DISCUSSION

The relation between the trace element abundances inferred from the EUV/soft X-ray emission and the effective temperature and surface gravity is best illustrated by a combined analysis of the *EXOSAT* and *IUE* data. We found that for a low abundance of trace elements relative to hydrogen, such as in GD 2 and EG 70, the optical/ultraviolet spectrum behaves independently of the chemical composition. Independent constraints on the effective temperature and the surface gravity are extracted in a first step from that spectral range. The issue of the chemical composition thus relies only on the EUV/soft X-ray photometric observations like those obtained with *Einstein* and *EXOSAT*. These observations do not allow a direct spectroscopic identification of the elements present but only the measurement of an integrated effect seen through the various count rates. The theory of diffusion offers the theoretical background that may help to draw a realistic picture of the atmospheric layers. Many physical processes play a role, or are suspected to play a role, in the atmosphere of those stars. Gravitational settling is the basic process that leads to the chemical separation of the hydrogen and the other elements. The effect of radiative forces acting on trace elements and a hypothetical mass loss might considerably modify the pure diffusive equilibrium of the chemical species.

It is in that context that Vennes *et al.* (1988) have studied the hydrogen/helium stratification of the atmospheric layers of the DA white dwarfs and that for example Chayer, Fontaine, and Wesemael (1989) have been led to postulate the existence of a weak wind affecting the behavior of the abundance pattern of the elements C, N, and Si in the hot DA stars Feige 24 and Wolf 1346. We have retained these two schemes as part of the theoretical framework behind the analysis of the EUV/soft X-ray emission of the DA white dwarfs, i.e, a stratified H/He composition and an arbitrary sample of metals uniformly distributed in the atmosphere. The next crucial step is to interpret the ultraviolet and EUV/soft X-ray data in a self-consistent model atmosphere analysis of the complete energy distribution of the DA white dwarfs in order to bring together the disparate pieces of information.

We have exposed, in the study of GD 2 and EG 70, some important conclusions with respect to these ideas. The analysis of the photometric *EXOSAT* data of GD 2 and EG 70 illustrates some basic difficulties encountered in the study of the EUV/soft X-ray photometry of the DA white dwarfs. For example, Paerels and Heise (1989) quoted upper limits to the abundance of homogeneous helium in the DA white dwarfs GD 71 (WD 0549+158) and GD 659 (WD 0050−332). But unlike the upper limits they found on other DA stars, these are temperature-dependent in the same fashion as the lower limits on the stratified H layer mass we find in the cases of GD 2 and EG 70: at the upper range of probable effective temperatures, trace elements are necessary to match the EUV/soft X-ray count rates. A consistent analysis of the ultraviolet data (*IUE*) and the EUV/soft X-ray data (*EXOSAT*) can help to constrain more effectively the atmospheric parameters in a case-by-case study. For example, we find that the case for GD 2 is not clear yet, as a small reddening effect and/or some uncertainties on the *IUE* flux calibration have implications on the determination of atmospheric parameters. There is at least one other DA white dwarf showing a similar behavior. The inferred interstellar hydrogen column density of GD 257 (WD 0548+000) is large enough (10^{20} cm^{-2}) to suggest a substantial reddening effect. The chemical structure of these two stars, GD 257 and GD 2, may remain uncertain until the effective temperature is more tightly constrained.

There is an intrinsic reason to reject in some cases the homogeneous H/He pattern. The DA star GD 2 exemplifies that situation. The *EXOSAT* photometric measurements lead to the rejection of a chemical composition pattern if no formal fit at 1 σ or 2 σ is obtained. For GD 2, using the grid of homogeneous H/He models at 46,000 K, there is a 3 σ discrepancy between the Lexan 3000 and the Al/P filter count rates. At the same temperature, the grid of stratified H/He models, provides an acceptable solution to the count rate analysis. It is attractive to see this as a direct confirmation of the hydrogen thin layer model, but we should stress that photometric analysis only provides weak evidence. The limited amount of information available in a photometric measurement, as well as the strong dependence of any theoretical interpretation on the accuracy of the filter effective areas at low energies, suggests caution.

Depending one one's view of the evolution of hot white dwarfs, there is another line of reasoning which can be used, in conjunction with the data reported here, to support the existence of a thin hydrogen layer in the DA white dwarfs. Years of searching have revealed that the hottest DA white dwarfs are stars like G191-B2B, with temperatures not exceeding 75,000 K (Holberg *et al.* 1989). While it is possible that something like nuclear burning can bring DA white dwarfs onto the white dwarf cooling sequence, though at higher temperatures (10^5 K), an alternative is that the direct progenitors of these stars are the DO/DAO white dwarfs.

The DO/DAO white dwarfs, at the highest temperatures, show weak He II features (the hot DO's), a combination of He II, He I, and H I features (the cool DOs), or a DA-like spectrum with weak He I and He II features at the lowest temperatures (the DAOs). One interpretation of these objects is that the total mass of hydrogen in their outer envelopes is fairly large, and that some as yet unknown, exotic effects prevent or

delay the separation of the H and He layers through gravitational settling. Another way of explaining the simultaneous visibility of H and He in these objects is to postulate that they have a thin hydrogen layer (log $M_H < -15$) on top of the helium envelope (see MacDonald and Vennes 1990 for a discussion). One could then interpret GD 2 as an evolved DO/DAO star, though our analysis seems to call for a somewhat thicker hydrogen layer with log $M_H = -13.5$. It is possible that the hydrogen in the DO/DAO stars has not all floated on the top. In this picture, the hydrogen layer is thickened by ongoing upward migration of hydrogen atoms from deep layers of the helium envelope and in which the total column opacity of the hydrogen layers is increased by the ongoing cooling of the star. However, we must stress that a complex of metals, like the one sketched for Feige 24 by Vennes *et al.* (1989), may account for the same observations of GD 2 and that a thin hydrogen layer may not be necessary. In that case, the link with possible C, N, and Si lines in the existing *IUE* high-resolution spectrum should be established. Indeed, both mechanisms, radiative support of metals and H/He stratification, may concur to provide the EUV/soft X-ray opacity needed in some cases.

Any further improvements in the determinations of the atmospheric parameters of the DA white dwarfs depend on the acquisition of more precise EUV/soft X-ray photometric measurements (with *ROSAT*) and of extended EUV spectrophotometric measurements enabling a direct spectroscopic identification of the trace elements (with *EUV Explorer*). High signal-to-noise ratio optical observations of the hydrogen Balmer lines may help to constrain the effective temperature and surface gravity of those stars and circumvent the effect of interstellar extinction. It may be necessary to improve the temperature scale of those stars via the development of an *IUE* ad hoc correction algorithm including the Lyα spectral range.

We wish to thank Elisabeth Poulin and Peter Thejll for many helpful comments on the processing of the data, Jim MacDonald for revising the manuscript, David Finley for providing details of the FBB correction algorithm, and Frits Paerels for his helpful collaboration. We would like also to thank the RDAF staff at NASA/GSFC for their assistance. We acknowledge support from grants NASA NAG 5-972 and NSF AST-87-20530.

REFERENCES

Auer, L. H., and Mihalas, D. 1972, *Ap. J. Suppl.*, **24**, 193.
Bohlin, R. C., and Grillmair, C. J. 1988, *Ap. J. Suppl.*, **68**, 487.
Chayer, P., Fontaine, G., and Wesemael, F. 1989, in *IAU Colloquium 114, White Dwarfs*, ed. G. Wegner (Berlin: Springer), p. 253.
Finley, D., Basri, G., and Bowyer, S. 1990, *Ap. J.*, **359**, 483 (FBB).
Fontaine, G., and Wesemael, F. 1987, in *IAU Colloquium 95, The Second Conference on Faint Blue Stars*, ed. A. G. Davis Philip, D. S. Hayes, and J. Liebert (Schenectady: L. Davis), p. 319.
Heber, U., Hunger, K., Jonas, G., and Kudritzki, R. P. 1984, *Astr. Ap.*, **130**, 119.
Heise, J., Paerels, F. B. S., Bleeker, J. A. M., and Brinkman, A. C. 1988, *Ap. J.*, **334**, 958.
Holberg, J. B., Kidder, K., Liebert, J., and Wesemael, F. 1989, in *IAU Colloquium 114, White Dwarfs*, ed, G. Wegner (Berlin: Springer), p. 188.
Holberg, J. B., Sandel, B. R., Forrester, W. T., Broadfoot, A. L., Shipman, H. L., and Barry, D. C. 1980, *Ap. J. (Letters)*, **242**, L119.
Holberg, J. B., Wesemael, F., and Basile, J. 1986, *Ap. J.*, **306**, 629 (HWB).
Jordan, S., and Koester, D. 1986, *Astr. Ap. Suppl.*, **65**, 367.
Jordan, S., Koester, D., Wulf-Mathies, C., and Brunner, H. 1987, *Astr. Ap.*, **185**, 253.
Kahn, S. M., Wesemael, F., Liebert, J., Raymond, J. C., Steiner, J. E., and Shipman, H. L. 1984, *Ap. J.*, **278**, 255.
Koester, D. 1989, *Ap. J.*, **342**, 999.
Koester, D., and Herrero, A. 1988, *Ap. J.*, **332**, 910.
Liebert, J., Fontaine, G., and Wesemael, F. 1987, *Mem. Soc. Astr. Italiana*, **58**, 17.
MacDonald, J., and Vennes, S. 1990, *Ap. J.*, submitted.
McCook, G. P., and Sion, E. M. 1987, *Ap. J. Suppl.*, **65**, 603.
Mihalas, D., Heasley, J. N., and Auer, L. H. 1975, NCAR Tech. Note TN/STR-104.
Morrisson, R., and McCammon, D. 1983, *Ap. J.*, **270**, 119.
Paerels, F. B. S., Bleeker, J. A. M., Brinkman, A. C., and Heise, J. 1988, *Ap. J.*, **329**, 849.
Paerels, F. B. S., and Heise, J. 1989, *Ap. J.*, **339**, 1000.
Petre, R., and Shipman, H. L. 1987, *Bull. AAS*, **19**, 1041.
Petre, R., Shipman, H. L., and Canizares, C. R. 1986, *Ap. J.*, **304**, 356.
Seaton, M. J. 1979, *M.N.R.A.S.*, **187**, 73P.
Shipman, H. L. 1976, *Ap. J. (Letters)*, **206**, L67.
Spitzer, L. 1978, *Physical Processes in the Interstellar Medium* (New York: Wiley).
Thompson, R. W. 1988, *NASA IUE Newsletter*, No. 35, p. 133.
Vennes, S. 1988, Ph.D. thesis, Université de Montréal.
Vennes, S., Chayer, P., Fontaine, G., and Wesemael, F. 1989, *Ap. J. (Letters)*, **336**, L25.
Vennes, S., Fontaine, G., and Wesemael, F. 1989, in *IAU Colloquium 114, White Dwarfs*, ed. G. Wegner (Berlin: Springer), p. 368.
———. 1990, in preparation.
Vennes, S., Pelletier, C., Fontaine, G., and Wesemael, F. 1988, *Ap. J.*, **331**, 876.
Vidal, C. R., Cooper, J., and Smith, E. W. 1973, *Ap. J. Suppl.*, **25**, 37.
Wesemael, F., Auer, L. H., Van Horn, H. M., and Savedoff, M. P. 1980, *Ap. J. Suppl.*, **43**, 159.

HARRY L. SHIPMAN and STÉPHANE VENNES: Department of Physics and Astronomy, Sharp Laboratory, University of Delaware, Newark, DE 19716

ROBERT PETRE: Laboratory for High Energy Astrophysics, Code 666, NASA/Goddard Space Flight Center, Greenbelt, MD 20771